*AAPS PharmSciTech, Vol. 15, No. 3, June 2014 (© 2014)*
DOI: 10.1208/s12249-014-0104-0

*Research Article*

# Fast Tablet Tensile Strength Prediction Based on Non-Invasive Analytics

**Anna Halenius,[1,2] Satu Lakio,[1] Osmo Antikainen,[1] Juha Hatara,[1] and Jouko Yliruusi[1]**

*Received 18 September 2013; accepted 23 February 2014; published online 18 March 2014*

***Abstract.*** In this paper, linkages between tablet surface roughness, tablet compression forces, material properties, and the tensile strength of tablets were studied. Pure sodium halides (NaF, NaBr, NaCl, and NaI) were chosen as model substances because of their simple and similar structure. Based on the data available in the literature and our own measurements, various models were made to predict the tensile strength of the tablets. It appeared that only three parameters—surface roughness, upper punch force, and the true density of material—were needed to predict the tensile strength of a tablet. Rather surprising was that the surface roughness alone was capable in the prediction. The used new 3D imaging method (Flash sizer) was roughly a thousand times quicker in determining tablet surface roughness than traditionally used laser profilometer. Both methods gave practically analogous results. It is finally suggested that the rapid 3D imaging can be a potential in-line PAT tool to predict mechanical properties of tablets in production.

**KEY WORDS:** 3D image analysis; modeling; PAT; surface roughness; tensile strength.

## INTRODUCTION

Compression process of tablets is influenced by the behavior of material and several compression parameters, which have a combined effect on the final product (1,2). With higher pressures, the particles tend to break down and then reorganize and/or plastically deform more efficiently during the compression. In addition, the moisture content of granules, particle size fraction, and lubricant concentration are factors affecting crushing strength.

Spectroscopic methods (Raman and near-infrared spectroscopies) have been used for the determination of mechanical strength of tablets (3–5). However, spectroscopies are indirect methods, and spectral data needs to be correlated by statistical analysis (6).

Ultrasonic and acoustic methods are considered direct and suitable tools for in-line tensile strength process analysis in tableting (6–8). With the real-time ultrasound measurements, it is even possible in theory to analyze the mechanical properties of tablets during compression (9). However, the measuring arrangements are still too demanding in practice.

Compression force mainly controls the surface characteristics. Therefore, accurate characterization of tablet surface roughness can give valuable information of the mechanical strength of tablets. In general, the smooth surface of a tablet indicates more contact points between particles inside the tablet resulting in a higher tensile strength.

For the measurement of surface roughness, atomic force microscopy (AFM) has a good spatial resolution, but possible scan size is relatively small (10,11). Confocal laser scanning microscope is limited to fluorescent materials. Also optical microscopy, laser profilometer (LP), and scanning electron microscopy (SEM) can be used for surface roughness measurements of tablets (11). Profilometers can provide data from larger scan sizes compared to AFM, but spatial resolution is not as good. The methods are not suitable for real-time measurements.

Many optical techniques have been used in studying surface roughness of solids. In 1993, Vorburger *et al.* (12) summarized a number of previous experiments on the measurement of the roughness of metallic surfaces by light scattering. Later, white light has been applied in studying surface in a microscopic range as well as with an extended field of view (13). The method was capable to determine the mean roughness from a few nanometers to several micrometers. In 2000, Wang *et al.* (14) developed a laser scattering technique to study surface roughness in submicrometer range. In addition, a diffractive optical element-based glossmeter and multivariate wavelet texture analysis are also promising tools to visualize surface texture (15,16).

Quality by design has been under extensive research since it can improve quality and increase productivity. Optical and electron microscopy and two-dimensional (2D) imaging have been widely used to analyze various pharmaceutically important surfaces. Combining 2D images obtained from different angles to create three-dimensional (3D) images has been considered a significant real-time process analysis tool. Granule size distribution has been determined in-line by

**Electronic supplementary material** The online version of this article (doi:10.1208/s12249-014-0104-0) contains supplementary material, which is available to authorized users.

[1] Division of Pharmaceutical Technology, Faculty of Pharmacy, University of Helsinki, P.O. Box 56 (Viikinkaari 5E)00014, Helsinki, Finland.
[2] To whom correspondence should be addressed. (e-mail: anna.halenius@helsinki.fi)

 

illuminating the sample from different angles using primary color lights and by determining the particle size from the 3D images taken (17). Later, basically the same technique was used in granule size determinations (18).

The crystal structures of sodium halides (NaF, NaCl, NaBr, and NaI) consist of simple face-centered cubics. These ionic compounds were selected as model materials, because ionic bonding is non-directional, and binding energy between ions logically decreases as the anion size increases. From traditionally used pharmaceutical materials, it would be rather challenging to get such a systematic and well-characterized set of materials. Pharmaceutical materials also often have polycrystalline forms, which does make controlling the compression behavior more difficult.

The prime purpose of this study was to create fast and user-friendly predictive models for tensile strength of tablets. The models were built by testing the effects of surface roughness and other easily quantifiable properties and to the tensile strength of tablets. In addition, the purpose was to compare two surface imaging techniques, *e.g.*, a non-contact laser profilometer (LP) and a new fast 3D-image analysis method (Flash sizer), which could be a potential in-line PAT tool to predict mechanical properties of tablets in production.

## MATERIALS AND METHODS

### Materials

The materials used in the study were analytical grades of sodium fluoride (NaF) (Riedel-de Haën, Seelze, Germany), sodium chloride (NaCl) (Riedel-de Haën), sodium bromide (NaBr) (Riedel-de Haën), and sodium iodide (NaI) (Merck, Darmstadt, Germany). Bulk materials were sieved to fraction 0.250–0.350 mm and stored in 35% relative humidity (RH).

### Material Properties

Physico-chemical properties of sodium halides *e.g.* melting point, anion radius, true density ($\rho_{true}$), Young's modulus, solubility *etc.* were collected from the literature. Altogether 33 different properties were composed (Supplement 1).

#### *Scanning Electron Microscopy*

Scanning electron microscopy (SEM) images (FEI Quanta 250 FEG, The Netherlands) were taken from powder samples. Before scanning, the samples were coated with platinum using a vacuum evaporator. SEM images were acquired at an accelerated voltage of 10 kV. Shape parameters (area, perimeter, roundness, elongation, equivalent diameter and major and minor axels) were calculated based on the SEM images using MATLAB software (v. 7.6 The MathWorks Inc., Natick, MA, USA).

### Tableting

The tablets were compressed in conditioned environment (22°C and 35% RH) with an instrumented eccentric tablet machine (Korsch EK0, Erweka Apparatebau, Hausenstamm, Germany). Flat-faced punches with a diameter of 9 mm were used, and the minimum distance between the upper and the lower punches was set to be 3.00 mm during the compression cycle of an empty tablet machine (*e.g.*, no powder in the die). Tablets were circular discs. The compression speed was 34 rpm. Suspension of 5% (*w*/*w*) magnesium stearate (Ph. Eur.) in acetone (Sigma Aldrich, Stenheim, Germany) was used as an external lubricant, and it was applied directly to the punches and die wall prior to each tablet compression. Lubrication was necessary to achieve compact tablets, although it was estimated to have a slightly smoothing effect. As the lubrication was not in the mass, it did not affect bond formation inside the tablet.

The die was filled manually with an accurately weighted amount of studied powder. The compression force was controlled by changing the amount of powder in the die. At first, the lowest amount of material that could form stable tablets was used. Thereafter, the amount of mass was gradually increased in the die, in order to achieve a higher compression force.

Each tablet was treated individually so that the properties of a single tablet, for example tensile strength and surface roughness, could be analyzed. Tablets were also marked so that their upper and lower faces could be distinguished at the roughness studies.

Tablet thickness was measured from the center of each tablet approximately 3–4 h after tableting by digital micrometer (Sony DZ 521, Sony, Tokyo, Japan). The results were used in the calculation of relative porosity of tablets and tensile strength.

The relative tablet porosity ($\phi$) was determined by using following equation:

$$\phi = 1 - \frac{\rho_{ave}}{\rho_{true}} \quad (1)$$

in which $\rho_{true}$ is the true density gained from the literature and $\rho_{ave}$ has been calculated by using the following equation:

$$\rho_{ave} = \frac{m}{V} \quad (2)$$

in which $m$ is tablet mass and $V$ is tablet volume.

The diametral crushing strength of the tablets was determined with a material tester (Lloyd LRX, Fareham, UK). Crushing strength was determined at 20±2°C and 35% RH. Crushing strength was converted into tensile strength ($\sigma_d$), because it is known to be a better indicator of mechanical strength, since it also takes into account the dimensions of tablets (6,19). For this purpose, following equation was used:

$$\sigma_d = \frac{2P}{\pi D t} \quad (3)$$

in which $P$ is the load needed to break the tablet, $D$ is the tablet diameter, and $t$ is the tablet thickness.

### Roughness of the Tablet Surface

#### *Non-Contact Laser Profilometry*

The roughness of tablet surfaces was determined from upper and lower faces by using non-contact laser profilometer (LP) (UBM Microfocus Optical Measuring System, UBM Messtechnik GmbH, Ettlingen, Germany). The measured

area was 2.5×2.5 mm. The resolution was 500 points/mm× 10 points/mm. One measurement took approximately 40 min. After data collection, the image was leveled to remove the slope caused by the tilting of the tablet surface using Ubsoft software (v. 2.8 DOS, UBM Messtechnik GmbH, Ettlingen, Germany). Average roughness (Ra) was calculated by using the following equation:

$$\mathrm{Ra} = \frac{1}{n}\sum_{i=1}^{n}\left|z_i - \overline{z}\right| \tag{4}$$

where $n$ is the number of points in the profile, $z_i$ is the $i$th individual measurement point, and $z$ is the average of all the points in the profile. Ra is the arithmetic average of the absolute values of the profile.

### *3D Surface Imaging*

Flash sizer (FS) set-up is represented in Fig. 1. Firewire CCD-camera (DMK 41BF02, The Imaging Source Europe GmbH, Bremen, Germany) with a resolution of 1,280×960 pixels was used for surface imaging of tablets. Tablet samples were put on the measuring table under the microscope (Leica MZ6 microscope, Leica Microsystems GmbH, Wetzlar, Germany). An accurately positioned light-emitting diode (LED) light sources (Luxeon TFFC K2 Star, 5027-PWC-10, LEDdynamics Inc, Randolph, VT, USA) illuminated the sample. The illumination system consisted of four LED lamps and lens assemblies (2/3" 55 mm Telecentric Lens, TEC-M55, Computar, Japan). A constant current power supply (BuckPuck, 3021-D-I-1000, LEDdynamics Inc, Randolph, VT, USA) was used in the study. In addition, microcontroller (ATmega168, Atmel Corporation, San Jose, CA, USA) was used to control light sources. The images were in 8-bit grayscale.

The tablet was illuminated from four directions according to Fig. 1. The light sources illuminated the tablet one after another, and the tablet was photographed straight from up simultaneously with illumination. This provided four images from each measurement, and the 3D surface of the tablet was calculated from these images (Fig. 1). This 3D image was used to calculate the roughness value for the tablet surfaces. Roughness value ($R_{\mathrm{FS}}$) was the arithmetic average of the absolute values of all points of the profile (20).

Depending on the angle of the illuminated surface spot, the brightness of each point on the surface varied due to surface roughness. The smaller the angle between the surface normal and light source the brighter the point on the surface. The angle of the surface was calculated using the brightness of each point on the surface because the brightness was measured from four different directions (four different light sources).

Photometric stereo-based method with four lights was used to obtain horizontal profiles and 3D surface of sample (18,21). Lights were placed 90° from each other to illuminate the surface of sample at an angle of 30°. Gradient field was calculated from an image using the following equations:

$$P_{i,j} = L_{i,j} - R_{i,j} \tag{5}$$

$$q_{i,j} = U_{i,j} - D_{i,j} \tag{6}$$

In Eqs. 5 and 6, $p_{i,\,j}$ is the approximation of surface gradient in horizontal direction at point $(i, j)$, $q_{i,\,j}$ is the approximation of surface gradient in vertical direction at point $(i, j)$, $L_{i,\,j}$ is the intensity of image at point $(i, j)$ when illuminated with left light, $R_{i,\,j}$ is the intensity of image at point $(i, j)$ when illuminated with right light, $U_{i,\,j}$ is the intensity of image at point $(i, j)$ when illuminated with up light, and $D_{i,\,j}$ is the intensity of image at point $(i, j)$ when illuminated with down light. Line integration of horizontal gradients was used in horizontal direction to obtain horizontal profiles of surface.

Line integration of vertical gradients was used in vertical direction to obtain vertical profiles of surface. Cumulative error typical in line integration-based methods was removed with high pass filter. It was assumed that sample surface was approximately straight on larger scale. High pass filter used was constructed from a moving average low pass filter. For each point $(i, j)$ in the final 3D surface, average height value of crossing horizontal and vertical profiles was used as height in point $(i, j)$. Roughness was calculated from the final 3D surface using Eq. 4.

FS was used to measure roughness and to obtain images of each tablet. The selected area from which roughness was measured was a rectangle with an area of 5×5 mm. One measurement took a few seconds.

## Modeling

At first stage, all parameters measured or gained from the literature were examined to find out which of them could predict the tensile strength of tablets. This was performed by calculating Pearson correlation coefficient between the tensile strength of tablet and each parameter.

In the next stage, the predictability of tensile strength was improved by using a multilinear regression model (MLR) in which two or more factors can predict tensile strength better than one factor alone. A principal component analysis (PCA) was used for choosing the correct factors for the MLR model. It was possible to identify correlating and dependent factors from each other with the help of the loading plot of the PCA.

New factors were included to the final MLR model as long as they improved the predictability of the model ($Q^2$). The coefficient of determination ($R^2$) increased as long as new factors were included to the model while the estimate of the predictive ability of the model ($Q^2$) did not increase after optimum number of factors was included to model but began to decrease (22). All modeling was performed by using Modde software (Modde for Windows 3.0, Umetrics, Umeå, Sweden).

## RESULTS

### Comparison of Laser Profilometer and Flash Sizer

The new Flash sizer (FS) method was compared to traditional non-contact laser profilometer (LP) method.

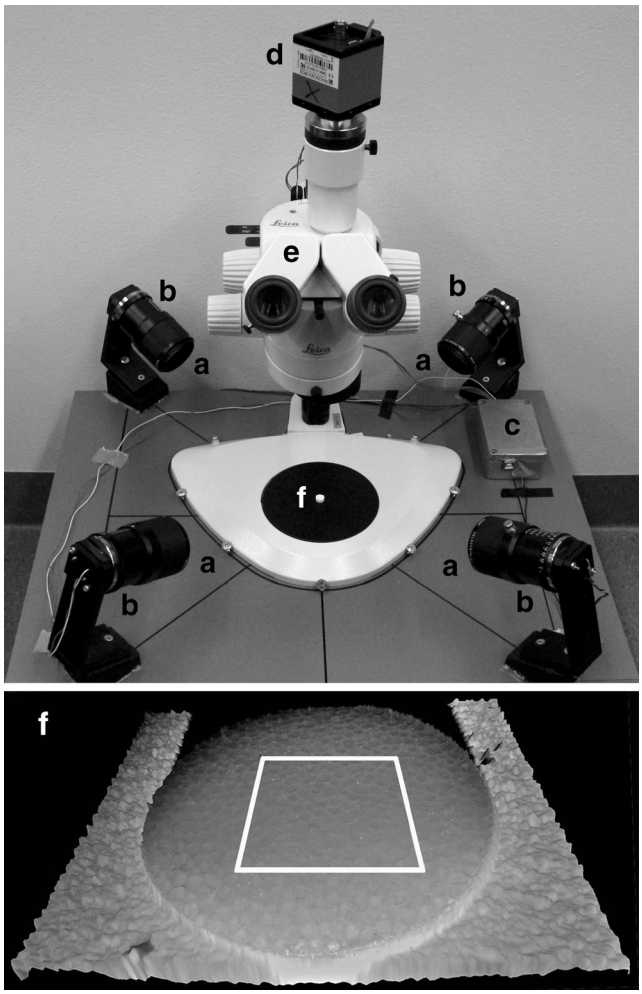


**Fig. 1.** Image analysis set-up. **a** Lenses for light sources, **b** LED light sources, **c** power source and automatic light controller, **d** CCD-camera, **e** microscope, and **f** tablet

Roughness values gained with these methods are referred to $R_{FS}$ and Ra, respectively.

To ensure that FS was a proper method for determining the surface roughness of tablets, roughness values (Ra and $R_{FS}$) were plotted against $F_{up}$ (Fig. 2). When $F_{up}$ increased, the roughness values decreased with all of the materials and with both of the methods. The roughness values were practically the same with upper and lower surfaces of the tablets. Thus, upper-side roughness values were used throughout the study. The roughness of the tablets complied with the periodic number of sodium halides: NaI formed the smoothest tablets while NaF formed the roughest tablets. The same simple exponential function was fitted to the data for every material (Fig. 2). Both of the methods gave similar results. NaF tablets measured with FS had less deviation with each other than those measured with LP.

$R_{FS}$ and Ra were also plotted against each other (Fig. 3), and a correlation was observed. The measured area with LP was quite small (2.5×2.5 mm) causing more deviation within the results. The plotted values in Fig. 3 seemed to behave a bit exponential manner. This was due to the fact that FS represented substantially rough surfaces more flat than LP because FS measured the surface with slant illumination, as for LP which gave the actual values (μm) for roughness. However, this did not seem to have a significant effect within the roughness range in tablet surfaces. Measurable roughness ranges are 0–500 μm for LP and 0–1,000 μm for FS.

As a conclusion, FS was found to be a suitable method for roughness measurements from surfaces of tablets. In addition, it was roughly thousand times faster than LP: one measurement took approximately 40 min with LP and only a few seconds with FS. FS is easy, non-invasive, and simple to use. The analyzed area is easily altered as well as other measuring parameters such as illumination time and angle of measurement. It is possible to use it for complicated surfaces such as tablets with logos, and it can also be used in the determination of particle size and film smoothness. Finally, FS does not require sample preparation and enables visual inspection of tablet surfaces in real-time revealing for instant flaws on the surface instantly. Based on these results, FS is supposed to be a suitable PAT tool.

## Modeling of the Tensile Strength of Tablets

Various factors from the literature and results gained in this study were modeled to predict the tensile strength of tablets ($\sigma_d$). The aim was that the factors in the model would be quickly measured or otherwise readily available so that the model would be suitable as a real-time PAT tool. In the first part of the study, principal component analysis (PCA) was used to choose possible factors for the model. The parameters were chosen in order to get the best prediction ability from all phases: material properties, compression data, and tablet properties. Thereafter, over 30 models were created. Next chapters will introduce the systematic set of eight most interesting and important models created using MLR (Model 1–Model 8) (Fig. 4). The $R^2$ and $Q^2$ parameters for the models are collected into Table I.

At first, $R_{FS}$ values were used to predict $\sigma_d$ (Model 1). Surprisingly, it appeared that $R_{FS}$ alone predicted $\sigma_d$ well (Fig. 5) ($R^2$=0.777, $Q^2$=0.734). The correlation between $R_{FS}$ and $\sigma_d$ seemed to behave exponentially. However, to further improve Model 1, another factor from the literature was introduced.

Totally, 33 physico-chemical properties of sodium halides from the literature (Supplement 1) were modeled in preliminary studies to predict $\sigma_d$. Most of the properties behaved according to the increasing periodic number of the halides as could be assumed. For instance, melting points of the sodium halides decreased when the ionic bond strength weakened: NaF 993°C, NaCl 801°C, NaBr 747°C, and NaI 661°C.

The most appropriate literature value found was true density ($\rho_{true}$) (results not shown). It was included for Model 2 which then had factors $R_{FS}$ and $\rho_{true}$ ($R^2$=0.905, $Q^2$=0.869). $\rho_{true}$ for NaI was 3.67 g/cm$^3$, NaBr 3.21 g/cm$^3$, NaCl 2.165 g/cm$^3$, and NaF 2.558 g/cm$^3$. To ensure that the materials used in this study had the same crystal structure, $\rho_{true}$ values were measured using helium pycnometer. The results strongly corresponded with the literature values. Tablets did not have individual values of $\rho_{true}$, since it is a material property. This has an effect on the predictive ability $Q^2$ of the model. However, the influence of $\rho_{true}$ was so significant that it improved the model.

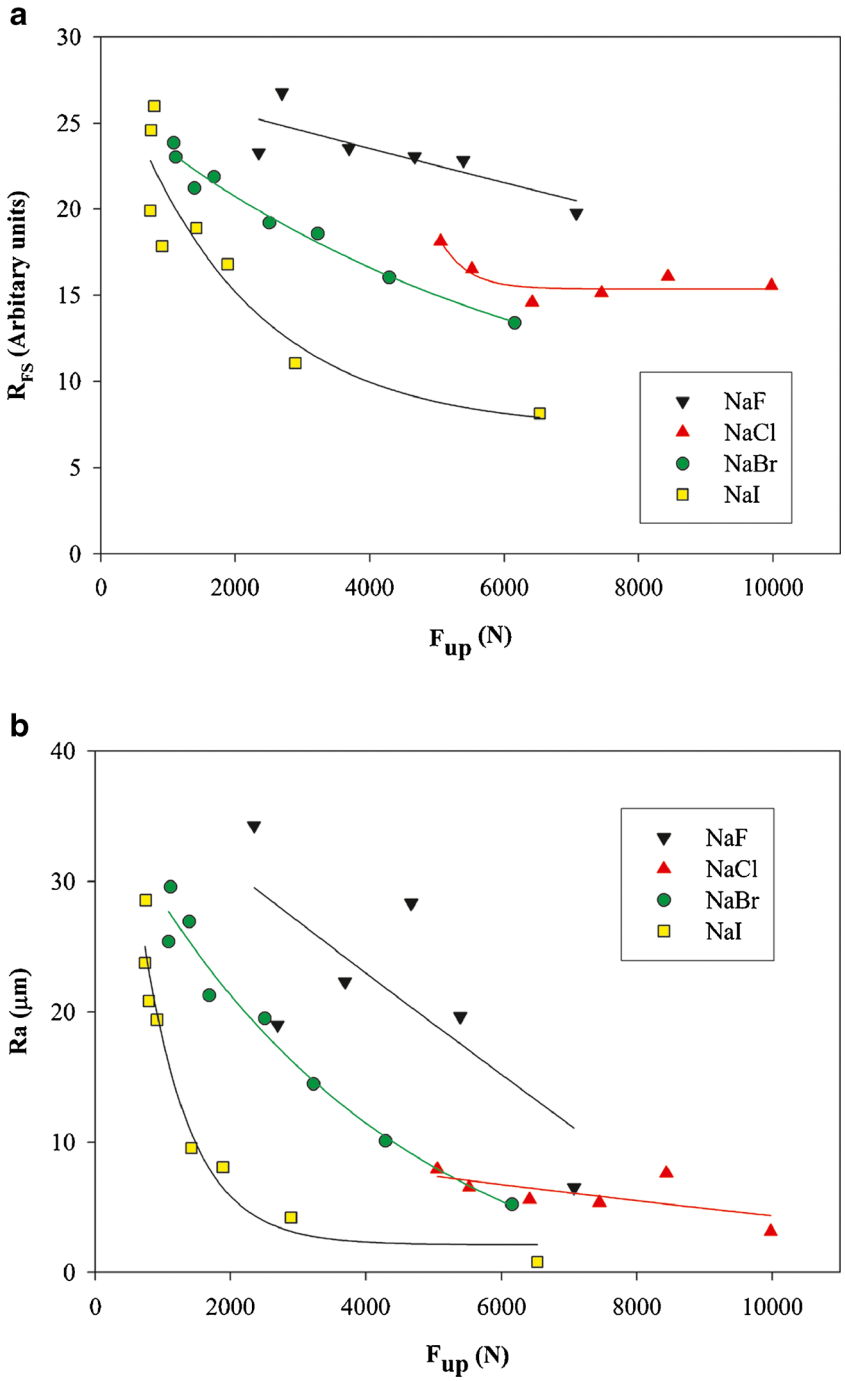


**Fig. 2.** Surface roughness plotted against maximum upper punch force ($F_{up}$). **a** Surface roughness ($R_{FS}$) measured with Flash sizer. **b** Surface roughness (Ra) measured with laser profilometer (LP)

It is important to notice that $\rho_{true}$ of the sodium halides did not correspond with the order of the periodic number; $\rho_{true}$ of NaF seemed to be higher than expected. As generally known, the electrons are very close to the nucleus inducing a higher electron density for NaF. The electron configurations of used halogens are represented in Supplement 2. Since $\rho_{true}$ is readily available, it enables real-time modeling. However, as supposed, $\rho_{true}$ cannot predict $\sigma_d$ alone. Thus, a new factor, the maximum upper punch force ($F_{up}$), was included in the model together with $\rho_{true}$ (Model 3) ($R^2$=0.857, $Q^2$=0.751). Parameters recorded during the compression phase are known to be important for mechanical strength of tablets (1,23). $F_{up}$ was found to be the most predictive factor of all compression parameters. $F_{up}$ can be recorded during the tableting, so it is available in real-time, and it is an excellent PAT parameter. It is known that $F_{up}$ can already alone predict $\sigma_d$ quite well (24,25). $R^2$ for this Model 4 was 0.064 and $Q^2$ −0.06. There were four materials in the model, and $F_{up}$ range

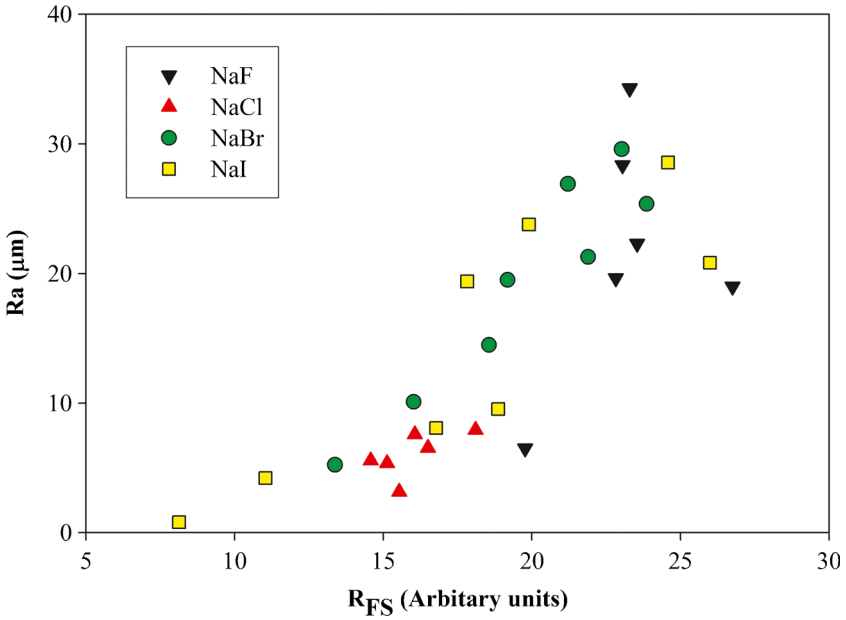


**Fig. 3.** Surface roughness scatter plot. Surface roughness values measured with Flash sizer ($R_{FS}$) and laser profilometer (Ra)

was quite different for every material. This explained the poor correlation between $F_{up}$ and $\sigma_d$. $F_{up}$ could predict $\sigma_d$ well within single sodium halide. A correlation between $F_{up}$ and $\sigma_d$ for each sodium halide is represented in Fig. 6. As generally known, $\sigma_d$ increased with increasing $F_{up}$.

Compactibility (the ability of the powdered material to be compressed into a tablet of specified strength) of the sodium halides behaved according to the periodic number. $F_{up}$ range for sodium halides was wide. In practice, it was possible to form tablets only in a narrow window about 5,000–6,000 N from all materials. There was a significant difference between the compactibility of the sodium halides. The highest compactibility was with NaI. NaCl was unable to form tablets under $F_{up}$ of 5,000 N. This suggested that no sufficient amount of bonds were formed between NaCl particles in lower forces. $F_{up}$ and $R_{FS}$ (Model 5) gave a $R^2$ of 0.854 and $Q^2$ 0.806, indicating a very good model. Model 5 was suitable for real-time determination of $\sigma_d$. However, thereafter, new factors were modeled to find even better prediction for $\sigma_d$.

According to the results, it seemed that also particle shape has an effect on $\sigma_d$. Particle shape parameters were determined based on SEM images (Fig. 7) taken in the same conditions in which tableting was performed. Several shape parameters were tested in the models. However, only *sphericity* could separate the sodium halides: highest sphericity was with NaCl and lowest with NaF. Thus, sphericity was chosen for two models including three factors. When sphericity, $\rho_{true}$, and $R_{FS}$ were modeled to predict $\sigma_d$, $R^2$ was 0.888 and $Q^2$ 0.841 (Model 6), and with sphericity, $F_{up}$, and $R_{FS}$, $R^2$ was 0.833 and $Q^2$ 0.767 (Model 7).

Finally, the best model (Model 8) included three factors: $R_{FS}$, $F_{up}$, and $\rho_{true}$ ($R^2$=0.923, $Q^2$=0.891). Predicted $\sigma_d$ using this model and measured $\sigma_d$ were plotted against each other (Fig. 8). There was a clear correlation between measured and

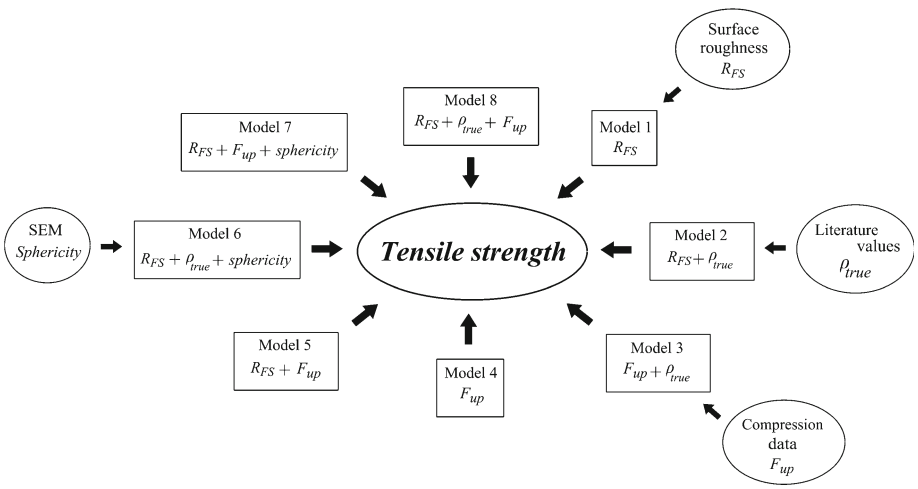


**Fig. 4.** Modeling of tensile strength of tablets. Models from 1 to 8 and factors included in these models. $R_{FS}$ surface roughness measured using Flash sizer, $\rho_{true}$ true density of sodium halide, $F_{up}$ maximum upper punch force, *sphericity* sphericity of sodium halide particles

**Table I.** The Models to Predict Tensile Strength of Tablets

| Model name | Number of factors | Factor(s) | $R^2$ | $Q^2$ |
|---|---|---|---|---|
| Model 1 | 1 | $R_{FS}$ | 0.78 | 0.73 |
| Model 2 | 2 | $R_{FS}+\rho_{true}$ | 0.91 | 0.87 |
| Model 3 | 2 | $F_{up}+\rho_{true}$ | 0.86 | 0.75 |
| Model 4 | 1 | $F_{up}$ | 0.06 | −0.06 |
| Model 5 | 2 | $R_{FS}+F_{up}$ | 0.85 | 0.81 |
| Model 6 | 3 | $R_{FS}+\rho_{true}$+sphericity | 0.89 | 0.84 |
| Model 7 | 3 | $R_{FS}+F_{up}$+sphericity | 0.83 | 0.77 |
| Model 8 | 3 | $R_{FS}+F_{up}+\rho_{true}$ | 0.92 | 0.89 |

$R_{FS}$ surface roughness measured using Flash sizer, $\rho_{true}$ true density of material, $F_{up}$ maximum upper punch force, *sphericity* sphericity of particles, $R^2$ the coefficient of determination, $Q^2$ the estimate of the predictive ability of the model

predicted $\sigma_d$ values. Within one material, $R_{FS}$ and $F_{up}$ were dependent of each other; but in the case of four different materials, they were independent. When using both $R_{FS}$ and $F_{up}$ in the model, the predictive ability of the model increased. $F_{up}$ provided information mostly from the compression process, but $R_{FS}$ included additional information of particle shapes, packing, and fragmentation of particles. True density appeared to be the best material property for differentiating materials in the models. $Q^2$ of this model was high indicating a good predictive ability of the model.

### Analysis of SEM Images

According to SEM (Fig. 7), the shape of NaF particles was irregular consisting of several cubical subunits. It was assumed that NaF particles broke down into subunits during compression with higher forces. Thus, NaF could mainly be a brittle material. $\sigma_d$ of NaF tablets was the lowest suggesting that bond formation between particles was not sufficient. The total number of contact points increased suggesting that the average attaching pressure between particles was so weak that additional bonds between the subunits could not be formed.

The habit of NaCl particles was very cubical. It was assumed that they need to organize side by side during compression to form bonds. This supposed also to cause higher deviation between tablet properties, such as tensile strength, depending how individual particles arranged during die filling. NaCl needed more force to form tablets than other sodium halides. This could also relate to the cubical shape: bond formation is hindered because contact points are limited between flat surfaces before particles reorganized and broke down into smaller, more irregularly shaped pieces. In addition, some of the NaCl tablets chipped during ejection, suggesting a hard material. NaCl is known to deform by fragmenting when compressing single particle, but behave plastically when compressing bulk mass.

The shape of NaBr was less cubical and more elongated than NaCl suggesting a more efficient packing in the mold compared to NaCl. $\sigma_d$ of NaBr was higher than NaCl indicating more contact points between particles and so more bonding. NaBr deformed more easily than NaCl.

NaI particles were more spherical than the other sodium halides, and the surfaces were soft-looking. This was partly explained with moisture adsorption. When the materials were conditioned with different humidities, it was noticed that NaI adsorbed water already at tableting conditions (35% RH) (results not shown). NaBr did not adsorb water at tableting conditions, and NaF and NaCl did not take water at all even with over 75% RH. Moisture content of the material did not improve the

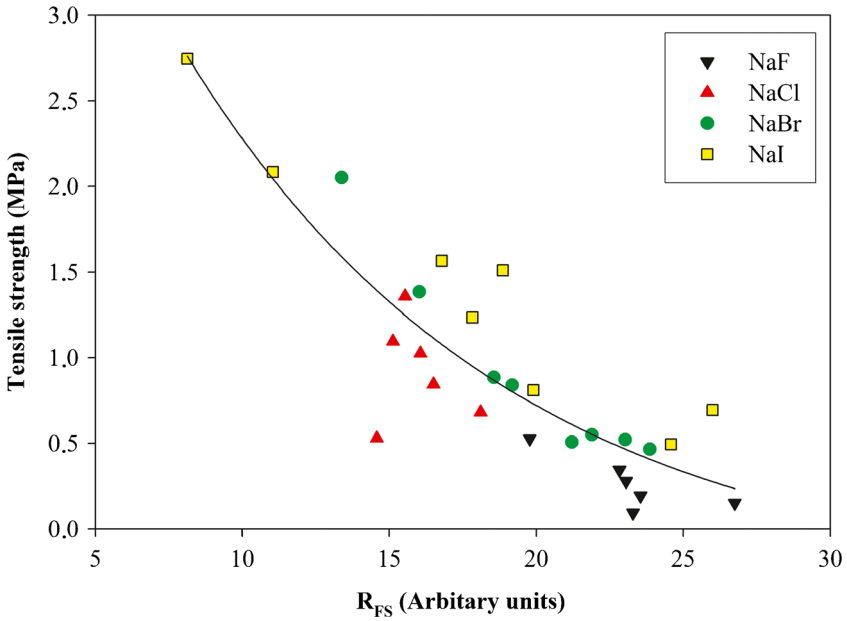


**Fig. 5.** Tensile strength of the tablets plotted against surface roughness measured with Flash sizer ($R_{FS}$)

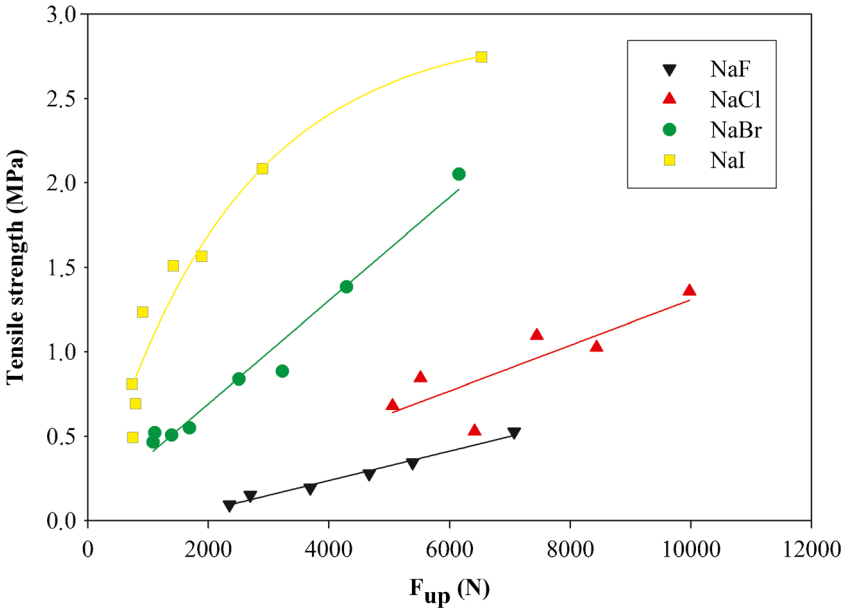


**Fig. 6.** Tensile strength of the tablets plotted against maximum upper punch force ($F_{up}$)

predictive ability of the model because it had an effect only on NaI. In addition, $\sigma_d$ was the highest with NaI. It is known that moisture can result in higher $\sigma_d$ until a certain material depended limit (26,27). It was assumed that NaI deformed mainly plastically due to a high moisture content.

### Relative Porosity

The relative porosity ($\phi$) of the tablets was expected to correlate well with $\sigma_d$. However, it could not be added to a MLR model because $F_{up}$ and $\phi$ were highly dependent from each other. $\phi$ range for tablets for NaI was 0.392–0.251, for NaBr 0.310–0.119, for NaCl 0.140–0.069, and for NaF 0.284–0.161. NaI formed the hardest tablets even if the $\phi$ of the tablets were the highest. It seemed that moisture increased the plasticity and $\sigma_d$ of the NaI tablets.

It also appeared that $\phi$ correlated with $\sigma_d$ within single sodium halide better than with the whole group. The order of $\phi$ did not comply with the periodic number of sodium halides. However, the porosity results corresponded with $\rho_{true}$ suggesting the influence of the difference in electron density of NaF also in the porosity results. In addition, according to SEM images, NaCl particles were very cubical whereas NaF particles were irregularly shaped. This morphological difference could have an effect on porosity of the sodium halides.

## DISCUSSION

Diametral crushing of tablets is a commonly used mechanical test. It is practical, but more problematic than usually supposed. During the last years, numerous simulations have been made in order to model and understand the mechanical properties of tablets (28–30). For example, with special 3D-DEM simulations, it was showed that the orientation of tablets in the crushing strength test significantly affects the obtained results (29). Thus, a vast variation in tablet crushing strength measurements even within the same tablet batch can greatly limit the predictability of tensile strength. Hence, a better model than Model 8 is quite impossible to achieve in practice.

It has been previously showed that surface roughness relates to the compression force, and it also includes additional information of particle shapes, packing, and fragmentation of particles (31). Roughness of a tablet surface has been seldom measured in-line mainly due to either slow data acquisition or small scan size. Used Flash sizer method is not hindered with these limitations. Currently, one determination can be done in a few seconds. However, we believe that the method can quite easily be further developed (electronics, calculation capacity, lights adjustment *etc.*) so that determination will take milliseconds. This would enable in-line measurements from tablet production line. Flash sizer has previously been considered a reliable and a possible PAT tool in pharmaceutical manufacturing processes (18).

Generally, predictive models include only one formulation in pharmaceutical applications. However, the models in this study were made for the whole group of sodium halides. Thus, including various materials in one model can give a more general understanding for the factors influencing the tensile strength of tablets. As a result, the functionality of the model was shown by its ability to cover these four different materials. For another set of materials or formulations, assumable other factors (particle shape, moisture content, viscoelasticity *etc.*) might be more relevant. For instance, it is known that moisture does have an effect on mechanical strength of other crystalline materials, and large differences in particle shape affect tensile strength of tablets (32,33). Furthermore, it was possible to use both $R_{FS}$ and $F_{up}$ in the same models only because the models were created for four sodium

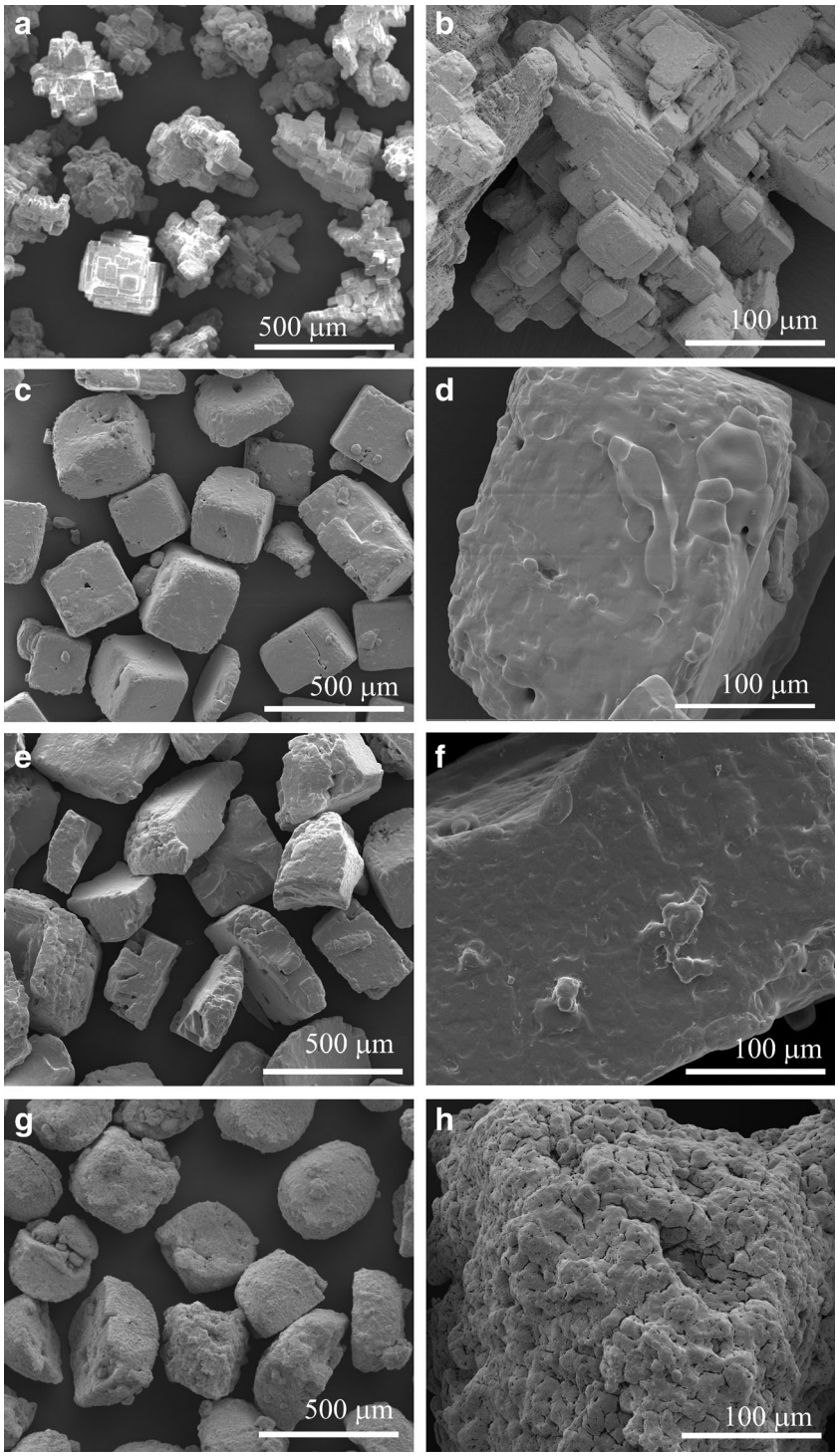


**Fig. 7.** SEM images of powders after 5 days storage in 35% RH. **a** and **b** NaF, **c** and **d** NaCl, **e** and **f** NaBr, **g** and **h** NaI

halides; but within one material, they are dependent of each other.

In the beginning, our purpose was to select a set of materials which were similar and as simple as possible. Thus, we chose sodium halides which have non-directional ionic bonding and simple cubic crystal lattice. However, it appeared that, for example, hygroscopicity of materials and particle morphology differed from each other considerably. Thus, even materials that seem simple at first sight are not that simple in real life.

## CONCLUSIONS

Only three parameters—surface roughness, upper punch force, and the true density of material—were needed to model the tensile strength of tablets. The surface roughness alone

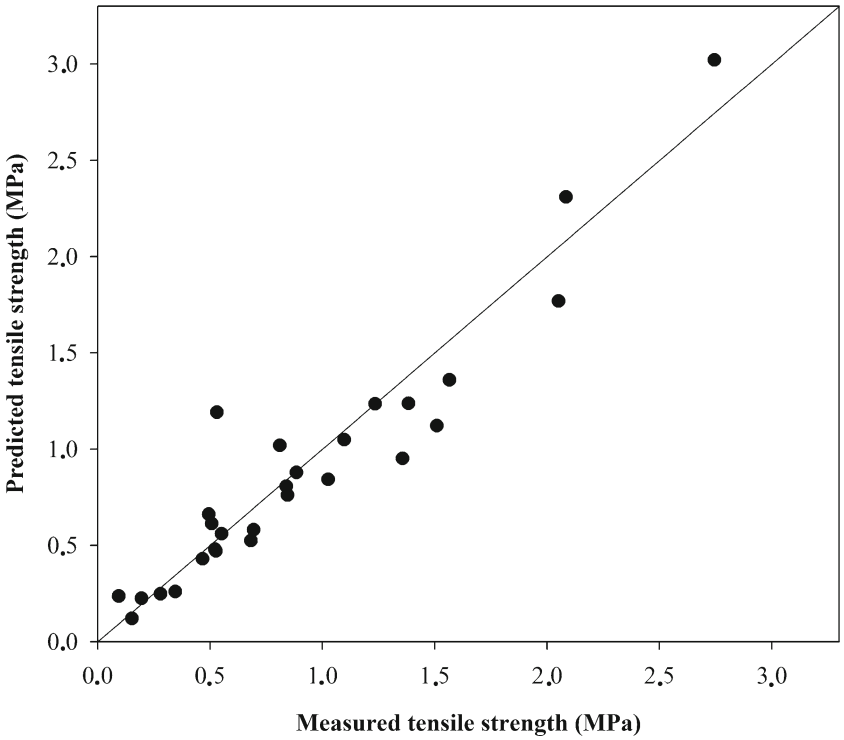


**Fig. 8.** Correlation between predicted and measured tensile strengths

was capable to predict the tensile strength of tablets surprisingly well. The used new 3D imaging method was significantly quicker in determining tablet surface roughness than the traditionally used laser profilometer. It is suggested that 3D surface imaging can be a potential in-line PAT tool to predict mechanical properties of tablets in production.

## REFERENCES


1. Bos CE, Bolhuis GK, Lerk CF, de Boer JH, Duineveld CAA, Smilde AK, *et al*. The use of a factorial design to evaluate the physical stability of tablets prepared by direct compression. I. A new approach based on the relative change in tablet parameters. Eur J Pharm Biopharm. 1991;37:204–9.
2. Sinka IC, Motazedian F, Cocks ACF, Pitt KG. The effect of processing parameters on pharmaceutical tablet properties. Powder Technol. 2009;189:276–84.
3. Gustafsson C, Nyström C, Lennholm H, Bonferoni MC, Caramella CM. Characteristics of hydroxypropyl methylcellulose influencing compactibility and prediction of particle and tablet properties by infrared spectroscopy. J Pharm Sci. 2003;92:494–504.
4. Tabasi SH, Fahmy R, Bensley D, O'Brien C, Hoag SW. Quality by design, part I: applications of NIR spectroscopy to monitor tablet manufacturing process. J Pharm Sci. 2008;97:4040–51.
5. Virtanen S, Antikainen O, Yliruusi J. Determination of the crushing strength of intact tablets using Raman spectroscopy. Int J Pharm. 2008;360:40–6.
6. Podczeck F. Methods for the practical determination of the mechanical strength of tablets—from empiricism to science. Int J Pharm. 2012;436:214–32.
7. Akseli I, Cetinkaya C. Air-coupled non-contact mechanical property determination of drug tablets. Int J Pharm. 2008;359:25–34.
8. Simonaho S-P, Takala TA, Kuosmanen M, Ketolainen J. Ultrasound transmission measurements for tensile strength evaluation of tablets. Int J Pharm. 2011;409:104–10.
9. Leskinen JTT, Simonaho S-P, Hakulinen M, Ketolainen J. Real-time tablet formulation monitoring with ultrasound measurements in eccentric single station tablet press. Int J Pharm. 2013;442:27–34.
10. Poon CY, Bhushan B. Comparison of surface roughness measurements by stylus profiler, AFM and non-contact optical profiler. Wear. 1995;190:76–88.
11. Seitavuopio P, Rantanen J, Yliruusi J. Tablet surface characterisation by various imaging techniques. Int J Pharm. 2003;254:281–6.
12. Vorburger TV, Marx E, Lettieri TR. Regimes of surface roughness measurable with light scattering. Appl Opt. 1993;32:3401–8.
13. Windecker R, Tiziani HJ. Optical roughness measurements using extended white-light interferometry. Opt Eng. 1999;38:1081–7.
14. Wang SH, Quan C, Tay CJ, Shang HM. Surface roughness measurement in the submicrometer range using laser scattering. Opt Eng. 2000;39:1597–601.
15. Juuti M, van Veen B, Peiponen K-E, Ketolainen J, Kalima V, Silvennoinen R, *et al*. Local and average gloss from flat-faced sodium chloride tablets. AAPS PharmSciTech. 2006;7(1):E1–6.
16. García-Muñoz S, Carmody A. Multivariate wavelet texture analysis for pharmaceutical solid product characterization. Int J Pharm. 2010;398:97–106.
17. Närvänen T, Seppälä K, Antikainen O, Yliruusi J. A new rapid on-line imaging method to determine particle size distribution of granules. AAPS PharmSciTech. 2008;9:282–7.
18. Soppela I, Airaksinen S, Hatara J, Räikkönen H, Antikainen O, Yliruusi J, *et al*. Rapid particle size measurement using 3D surface imaging. AAPS PharmSciTech. 2011;12:476–84.
19. Fell JT, Newton JM. The tensile strength of lactose tablets. J Pharm Pharmacol. 1968;20:667–8.
20. Krogars K, Antikainen O, Heinämäki J, Laitinen N, Yliruusi J. Tablet film-coating with amylose-rich maize starch. Eur J Pharm Sci. 2002;17:23–30.
21. Woodham RJ. Photometric method for determining surface orientation from multiple images. Opt Eng. 1980;19:139–44.

22. Eriksson L, Johansson E, Kettaneh-Wold N, Trygg J, Wikström C, Wold S. Multi- and megavariate data analysis part I: basic principles and applications. Umeå: Umetrics Academy; 2006.
23. Lindberg N-O, Jönsson C, Holmquist B. Optimization of disintegration time and crushing strength of a tablet formulation. Drug Dev Ind Pharm. 1985;11:931–43.
24. Antikainen O, Tervakangas H, Pietiläinen J, Yliruusi J, Sandler N. Screening of particle size related segregation behavior of granules with surface image analysis. AAPS 2006; J8.
25. Virtanen S, Antikainen O, Räikkönen H, Yliruusi J. Granule size distribution of tablets. J Pharm Sci. 2010;99:2061–69.
26. Khan F, Pilpel N, Ingram S. The effect of moisture on the density, compaction and tensile strength of microcrystalline cellulose. Powder Technol. 1988;54:161–4.
27. Malamataris S, Goidas P, Dimitriou A. Moisture sorption and tensile strength of some tableted direct compression excipients. Int J Pharm. 1991;68:51–60.
28. Procopio AT, Zavaliangos A. Simulation of multi-axial compaction of granular media from loose to high relative densities. J Mech Phys Solids. 2005;53:1523–51.
29. Siiriä S-M. Towards understanding powder behavior via simulation [dissertation]. Helsinki: University of Helsinki; 2011.
30. Podczeck F, Drake KR, Newton JM. Investigations into the tensile failure of doubly-convex cylindrical tablets under diametral loading using finite element methodology. Int J Pharm. 2013;454:412–24.
31. Narayan P, Hancock BC. The relationship between the particle properties, mechanical behavior, and surface roughness of some pharmaceutical excipient compacts. Mater Sci Eng A. 2003;355:24–36.
32. Ahlneck C, Alderborn G. Moisture absorption and tableting. I. Effect on volume reduction properties and tablet strength for some crystalline materials. Int J Pharm. 1989;54:131–41.
33. Obae K, Iijima H, Imada K. Morphological effect of microcrystalline cellulose particles on tablet tensile strength. Int J Pharm. 1999;182:155–64.